Int. J. Heat Mass Transfer. Vol. 25, No. 5, pp. 653–660, 1982
Printed in Great Britain

0017–9310/82/050653–08 $03.00/0

SEMI-EMPIRICAL THEORY OF FILM CONDENSATION OF PURE VAPOURS

S. S. KUTATELADZE
Institute of Thermophysics, Siberian Branch of the U.S.S.R. Academy of Sciences, Novosibirsk, U.S.S.R.

(*Received* 27 *October* 1981)

Abstract—Some simple mathematical models of film condensation of pure non-metal vapours are discussed and their correction according to the available experimental data is described.

NOMENCLATURE

a, diffusivity of condensate heat [m^2/s];
Ar_*, Archimedean number, equation (3);
C, heat capacity coefficient of condensate [J/kg K];
C_f'', friction coefficient of vapour on condensate surface;
Fr, Froude number, equation (6);
G, mass flow rate of condensate per unit width of cooling surface (wall) [kg/m s];
$\bar{j}''$, relative fluid momentum to interphase, equation (9);
K, thermal similarity number in type I phase transition, equation (5);
L_1, total height of wall [m];
Nu^*, Nusselt number, equation (1);
Pr, physical Prandtl number, equation (4);
q, q_w, heat flux density on vapour–liquid interface and on wall surface, respectively;
Re, Reynolds number of condensate film, equation (2);
Re'', Reynolds number, equation (8);
r, latent heat of vaporization [J/kg];
T'', T_w, saturation and cooling surface temperature, respectively [K];
$\bar{t}$, $= \langle U\rangle t/\langle\delta\rangle$, dimensionless time (hydrodynamic homochromatic number);
U'', vapour flow velocity along interphase [m];
u, longitudinal velocity component of condensate flow [m];
v_w^*, dynamic velocity on wall [m];
We, Weber number, equation (27);
X, coordinate directed streamwise along vertical condensate flow [m];
$\bar{X}$, $x/\langle\delta\rangle$, dimensionless longitudinal coordinate;
Y, coordinate directed normally from wall to interphase [m];
Y, $= Y/\langle\delta_0\rangle$, dimensionless transverse coordinate.

Greek symbols

α, $= q_w/(T''' - T_w)$, heat transfer coefficient [B_T/m^2 K];
δ, condensate film thickness [m];
δ', $= \delta/\langle\delta\rangle$, relative perturbation in liquid film thickness;
ε, exponent of Pr, equation (18);
η, $= V_w^* Y/\nu$, dimensionless distance from wall (local Reynolds number);
η_δ, the same as at $Y = \delta$;
λ, thermal conductivity coefficient of condensate [B_T/m K]
μ, dynamic viscosity of condensate [HC/m^2];
ν, kinematic viscosity of condensate [m^2/s];
ρ', ρ'', condensate and vapour density, respectively [kg/m^3];
σ, surface tension coefficient on vapour–condensate interphase [H/m];
τ, τ_w, current and wall shear stress, respectively [H/m^2];
ϕ, relative influence of condensate supercooling, equation (13).
$\overline{\Delta\rho}$, $= (\rho' - \rho'')/\rho''$, relative difference in phase densities;
δ_σ, number of geometrical similarity, equation (7);

Subscripts

cr, critical;
l, laminar;
lw, laminar wave;
T, turbulent;
Tw, turbulent wave;
w, wall;
δ, external boundary of liquid film.

SIMILARITY CRITERIA

IN FILM condensation of pure non-metal sufficiently dense gases the thermal resistance is practically concentrated in liquid phases. Hence, at all points of the liquid–vapour interphase the temperature equals that of saturation T'', and on the cooling surface either the temperature T_w or the heat flux density q_w are specified.

A mechanical interaction on the interphase is determined by the relative motion of phases, the flow

density of vapours condensing on this interphase, the surface tension and the character of arising waves.

The respective similarity criteria can be written in the following forms [1]:

the Nusselt number constructed according to the gravitational–viscous linear scale as

$$Nu^* = \frac{\alpha}{\lambda}\left(\frac{\nu^2}{g\Delta\rho}\right)^{1/3}, \tag{1}$$

the Reynolds number of the condensate as

$$Re = G/\mu, \tag{2}$$

the Archimedes number, constructed according to the capillary–gravitational linear scale, as

$$Ar_* = \frac{\sigma^{3/2}}{\mu^2 g^{1/2}(\rho' - \rho'')^{3/2}}, \tag{3}$$

the Prandtl number of the condensate as

$$Pr = \frac{\nu}{a}, \tag{4}$$

the number of thermal similarity of type 1 physico-chemical conversions as

$$K = \frac{r}{C(T'' - T_w)}, \tag{5}$$

The similarity number of the friction interaction with the gravitational effect on the interphase (the generalized Froude number) as

$$Fr = \frac{C_f'' \rho'' V''^2}{Lg(\rho' - \rho'')}, \tag{6}$$

the relation for the linear scales of the capillary–gravitational interaction and of the cooling surface as

$$\delta_\sigma = L^{-1}\left[\frac{\sigma}{g(\rho' - \rho'')}\right]^{1/2}. \tag{7}$$

In the general case the effective coefficient of vapour friction on the condensate surface C_f'' depends upon the vapour Reynolds number,

$$Re'' = \frac{U''L}{\nu}, \tag{8}$$

and on the relative mass flow through the interphase,

$$\overline{j''} = \frac{q_\delta}{r\rho''u''}, \tag{9}$$

at

$$\overline{j''} > C_{f_0}'', \quad C_f'' \approx \overline{j''}. \tag{10}$$

Here C_{f_0}'' is the "dry" friction coefficient.

LAMINAR FLOW OF CONDENSATE WITH UNPERTURBED (SMOOTH) INTERPHASE

This classical problem was formulated and mainly solved by Nusselt [2].

For a vertical cooling surface and slowly moving vapour, when the interface friction can be neglected, the respective formulas are of the form:

$$\begin{matrix} T_w = \text{const.} \\ q_w = \text{const.} \end{matrix} \qquad Nu^* = (3Re)^{-1/3}, \quad (K \gg 1). \tag{11}$$

Respectively,

$$\langle Nu^* \rangle = ARe^{-1/3}. \tag{12}$$

At $T_w = \text{const.}$, $A = 0.92$; at $q_w = \text{const.}$, $A = 1.04 \approx 1$. Averaging was made from the upper edge of the cooling surface where $Re = 0$, to the given Reynolds number of the condensate film.

The effect of condensate supercooling is taken into account via the introduction of the effective condensation heat:

$$r_* = r(1 + \phi K^{-1}). \tag{13}$$

In the Nusselt problem $\phi = 3/8$. The geometry slightly influences the numerical coefficient of this theory. A solution for the moving vapour is tabulated in terms of the similarity criteria:

$$\frac{\alpha}{\alpha_0}; \quad \frac{C_f u''^2 \rho'' \langle \alpha_0 \rangle}{g\rho'\lambda} \tag{14}$$

where α_0 is the heat transfer coefficient at $U'' = 0$.

TURBULENT CONDENSATE FLOW WITH UNPERTURBED (SMOOTH) INTERPHASE

The problem of turbulent vapour condensation was simultaneously formulated by Kirkbredt [3] on the purely empirical basis and by Colborn [4] in terms of the Reynolds analogy between heat transfer and friction with the application of numerical coefficients found for channel flows. Consideration of this problem in terms of the classical semi-empirical turbulent boundary Prandtl layer theory was first performed by the author [5]. But, as with subsequent studies by other researchers, proper attention was not given to the qualitative difference in the problems of the heat transfer in liquid film cooling without phase transitions and of the film vapour condensation.

In the former case the heat flux is distributed so that on the external film boundary it is equal to zero, whereas on the cooling surface its value is maximum. Thus the turbulent transfer conditions in a viscous sublayer and its immediate vicinity are well defined. Hence it is unnecessary to give here detailed transfer conditions for the greater part of the flow on the side of a free liquid boundary.

In the latter case the heat flux through a liquid film is either practically constant ($\phi K^{-1} \ll 1$) or changes insignificantly. Therefore, the turbulent transfer mechanisms are essential at all points of the condensate film. In this latter case the main integral equation is of the form

$$Nu_T^* = \eta_\delta^{1/3}\left(\int_0^{\eta_\delta} \frac{d\eta}{1 + \varepsilon Pr\tilde{\mu}_T}\right)^{-1}, \tag{15}$$

$$\langle Nu^* \rangle = (\eta_\delta - \eta_{\delta cr})^{-1} \int_{\eta_{\delta cr}}^{\eta_\delta} Nu_T^* \, d\eta_\delta. \tag{16}$$

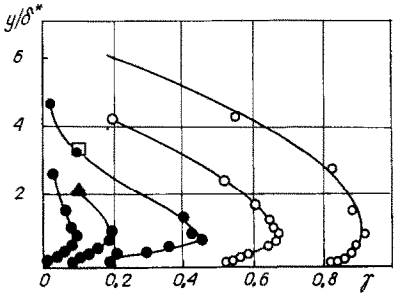

FIG. 1. Changes in the intermittence coefficient γ over the boundary layer thickness (δ^*—thickness of repulsion) in the laminar–turbulent boundary layer transition (according to the data by Tetyanko).

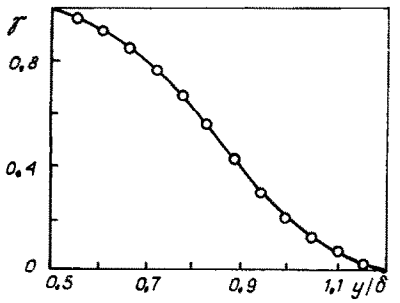

FIG. 2. Changes in the intermittence coefficient γ over the boundary layer thickness (δ—calculated thickness of the boundary layer).

The coefficient ε at large Re is equal to the inverse value of the turbulent Prandtl number

$$Pr_T = \frac{C\mu_T}{\lambda_T}; \quad Re \gg Re_{cr} \quad \varepsilon \approx Pr_T^{-1}. \tag{17}$$

In the region of the laminar–turbulent transition, this coefficient can account for the effect of intermittence, i.e. alternate transition of laminar and turbulent formations (units) through a given cross-section of the film.

Values and character of the change in the intermittence coefficient in the region of the developed turbulent boundary layer of a noncompressible liquid on the plate can be determined according to the data from Figs. 1 and 2.

In the general case,

$$\varepsilon = \varepsilon(Re; \bar{y}; Pr; Ar_*), \tag{18}$$

the main arguments are the Reynolds number and the relative distance from the wall.

For the classical Prandtl two-layer model typical for the near-wall region of the turbulent boundary layer, we have

$$\left.\begin{aligned} 0 < y < 11.6\,\nu/v_w^*, \quad & \mu_T = 0 \\ y > 11.6\,\nu/v_w^*, \quad & \mu_T = 0.16\,\rho' y^2 \frac{du}{dy} \end{aligned}\right\}. \tag{19}$$

for a free vertical flow the wall dynamic velocity is

$$v_w^* = (g\delta\bar{\Delta}\rho)^{1/2}, \tag{20}$$

and the shear stress distribution over the film thickness is linear

$$\tau = \tau_w(1 - \bar{y}). \tag{21}$$

The respective solution at Pr = const. is of the form

$$Nu^* \approx 0.4\,\overline{Pr}\,\eta_\delta^{1/3}\left(\ln\frac{\sqrt{\eta_\delta}+\sqrt{(\eta_\delta-11.6)}}{\sqrt{\eta_\delta}-\sqrt{(\eta_\delta-11.6)}} + 4.65\,Pr\right)^{-1}. \tag{22}$$

Here $Pr = \varepsilon\,Pr$ and the film Reynolds number is:

$$Re \approx \eta_\delta(3.0 + 2.5\ln\eta_\delta) - 39. \tag{23}$$

Data of the calculations according to the above formulas are given in Table 1.

A fairly good agreement with experimental data was obtained via the introduction of the deliberately decreased critical value of the condensate film Reynolds number $Re_{cr} = 100$.

A much more detailed description for the hydrodynamics over the total thickness of the fully developed turbulent boundary layer is provided by a scheme wherein the turbulent viscosity is partly approximated by the equations.

$$\left.\begin{aligned} 0 < \eta < 6.8, \ \bar{\mu}_T = 0; \\ 6.8 < \eta < 6.8 + 0.2(\eta_\delta - 6.8) = 5.44 + 0.2\,\eta_\delta; \\ \bar{\mu}_T = 0.4(\eta - 6.8)\sqrt{\left(1 - \frac{\eta}{\eta_\delta}\right)}; \\ 5.44 + 0.2\,\eta_\delta < \eta < \eta_\delta, \\ \bar{\mu}_T = 0.08(\eta - 6.8)\sqrt{\left(1 - \frac{\eta}{\eta_\delta}\right)}. \end{aligned}\right\} \tag{24}$$

In this scheme the mixing length outside the viscous sublayer is measured from its conventional boundary $\eta = 6.8$ correlating with the Prandtl–Karmann constant $\alpha = 0.4$ [6] and the relationship $\eta = \bar{y}$ in (21).

Integrals (15) in these expressions for $\bar{\mu}_T$ and $\overline{Pr} \approx$ const. are taken in quadratures. The latters are, however, cumbersome and the direct numerical calculation is more simple.

Table 1. Local values of Nu_T^* according to model (19)

η_δ	Re	Nu_T^* $\overline{Pr} = 1$	$\overline{Pr} = 1.75$	$\overline{Pr} = 3$	$\overline{Pr} = 5$
15	103	0.175	0.189	0.198	0.204
30	307	0.186	0.213	0.232	0.246
50	590	0.200	0.238	0.266	0.284
60	757	0.206	0.249	0.280	0.300
100	1410	0.230	0.280	0.321	0.350
200	3210	0.266	0.333	0.388	0.430
300	5140	0.288	0.367	0.430	0.482
1000	20,200	0.381	0.500	0.610	0.690
4000	94,500	0.534	0.723	0.900	1.04
7000	176,000	0.615	0.842	1.06	1.24
20,000	555,000	0.827	1.14	1.45	1.71

Table 2. Local values of Nu_T^* according to model (24)

$\overline{Pr}$	$\eta_\delta = 30$	50	60	100	200	300	1000	4000
1	0.160	0.157	0.158	0.164	0.181	0.195	0.255	0.359
2	0.198	0.209	0.215	0.236	0.275	0.303	0.411	0.588
3	0.226	0.247	0.257	0.289	0.343	0.382	0.527	0.858
5	0.265	0.300	0.315	0.361	0.438	0.491	0.690	0.996
7	0.292	0.336	0.354	0.410	0.501	0.565	0.801	1.155
10	0.320	0.372	0.393	0.459	0.566	0.640	0.917	1.316
Re	236	504	652	1280	3020	4900	19,700	94,750

Table 3. Values of $\langle Nu_T^* \rangle$ according to model (24)

$\overline{Pr}$	$\eta_\delta = 60$	100	200	300	1000	4000	Lower limit
1	0.157	0.160	0.168	0.176	0.213	0.285	$\eta_\delta = 50$
2	0.212	0.223	0.245	0.262	0.332	0.452	
3	0.252	0.270	0.300	0.324	0.416	0.572	
5	0.307	0.332	0.377	0.410	0.532	0.735	
7	0.344	0.374	0.428	0.467	0.607	0.841	
10	0.382	0.418	0.479	0.523	0.682	0.948	
Re	652	1280	3020	4900	14,700	94,750	

Table 2 represents the respective data for Pr = const.

As seen, the second model provides a weaker effect of the film Reynolds number in the region of its low values. By increasing the Reynolds number, calculations according to the both models correlate.

Table 3 represents mean values of the Nusselt number in the range from the critical to the given Reynolds number.

Figure 3 illustrates the $\{\langle Nu^* \rangle; \overline{Pr}\}$ dependences plotted for five values of the Reynolds number of the condensate film. As seen in the region of $\overline{Pr} \approx 1$ this dependence becomes rather weak.

Figure 4 illustrates the plotted dependences of the local Nu^* values calculated in the laminar and the turbulent regions according to the Nusselt formula and Table 2, respectively. Figure 5 respresents similar plots for the Nusselt number averaged over the turbulent flow region and over the total flow with laminar and turbulent regions according to the simple equation:

$$\langle Nu^* \rangle = \langle Nu_l^* \rangle \frac{Re_{cr}}{Re} + \langle Nu_T^* \rangle \frac{Re - Re_{cr}}{Re}. \quad (25)$$

It is seen that the effect of the laminar region of the condensate flow practically degenerates at $Re > 5000$.

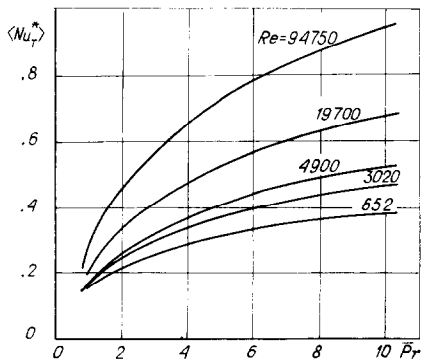

FIG. 3. Dependence of $\langle Nu_T^* \rangle$ upon Pr and Re according to Table 3.

LAMINAR WAVE CONDENSATE FLOW

Real flows of liquid films are of the wave character. The waves on their surface have different structures and they exert different influence on the averaged flow and the heat and mass transfer in laminar and turbulent flows.

For a vertical wall a 2-dim. laminar wave liquid film flow with a free boundary is described by the model Kapitsa–Nakoryakov equation [6–8]

$$\left(\frac{\partial}{\partial \bar{t}} + \frac{\partial}{\partial \bar{x}}\right)\bar{\delta}' + \frac{Re}{3}\left(\frac{\partial}{\partial \bar{t}} + 1.69\frac{\partial}{\partial \bar{x}}\right)\left(\frac{\partial}{\partial \bar{t}} + 0.71\frac{\partial}{\partial \bar{x}}\right)\bar{\delta}'$$
$$+ We\frac{\partial^4 \bar{\delta}''}{\partial \bar{x}^4} + 6\bar{\delta}'\frac{\partial \bar{\delta}'}{\partial \bar{x}} + \frac{2}{5}Re\frac{\partial}{\partial \bar{x}}\left(\bar{\delta}'\frac{\partial \bar{\delta}'}{\partial \bar{t}}\right) = 0 \quad (26)$$

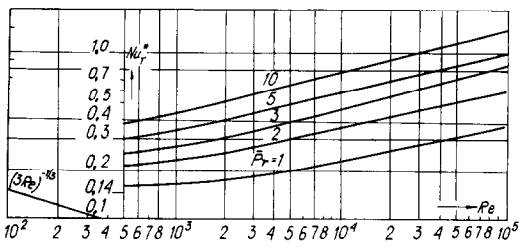

FIG. 4. Dependence of local values of Nu^* upon Pr and Re. Laminar region—Nusselt data; turbulent region—Table 2.

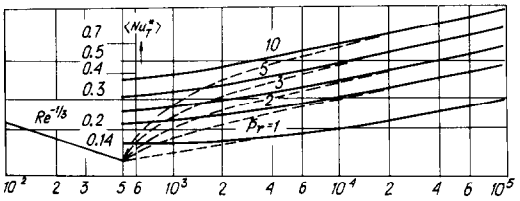

FIG. 5. Dependence of $\langle Nu^* \rangle$ upon Pr and Re according to (25). Laminar region—Nusselt data, turbulent region—Table 2.

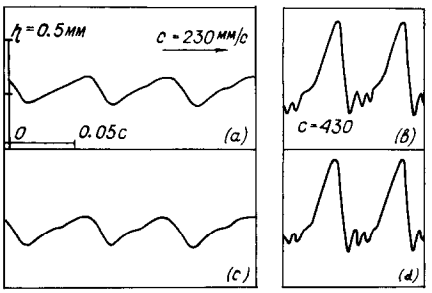

FIG. 6. Two-dimensional steady natural (a, b) and excited (c, d) waves of the same frequency. (a, b)—$Re = 7.6$; (c, d)—$Re = 22.7$.

here

$$We = \frac{\sigma}{\rho \langle \delta \rangle \langle u_\delta^2 \rangle}. \tag{27}$$

Not going into the details of the well known solutions of this equation, we will note only that it leads to the existence of a so-called "residual layer" whose thickness is slightly dependent upon the total consumption of the vertical liquid flow. This fact was, apparently, revealed by Brauer [9].

Profiles of the 2-dim. waves arising spontaneously (natural) and specially excited [8] are illustrated in Fig. 6. Figure 7 represents the pictures of real 3-dim. waves arising on liquid surfaces in film vapour condensation.

The thermal resistance of the condensate between the waves is determined by the thickness of the "residual layer" δ_0, i.e. in the laminar regime in these flow regions the heat transfer intensity is of the order

$$Nu^* \approx \frac{\nu^{2/3}}{\delta_0 (g\Delta\rho)^{1/3}} \approx \text{const}. \tag{28}$$

This is the explanation for the Re region where the heat transfer is quasi-self-similar in the film condensation of a pure slowly moving vapour [10, 11].

According to the Brauer data for a vertical wall, the laminar flow of a film with a smooth surface transforms into the laminar wave at

$$Re_{lw} \approx 2{,}3(Ar_*)^{1/5}, \tag{29}$$

which in turn transforms into a turbulent wave at

$$Re_{Tw} \approx 35(Ar_*)^{1/5}. \tag{30}$$

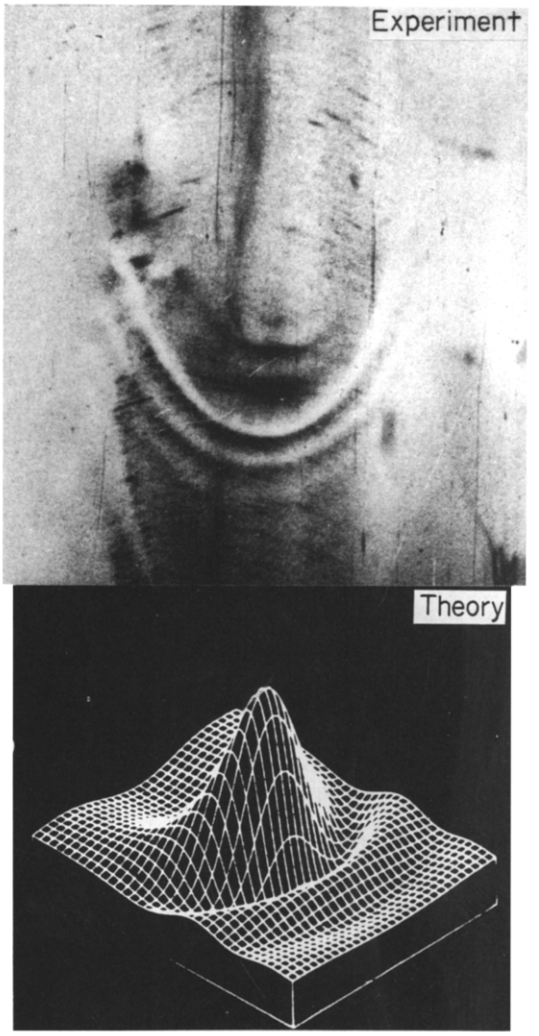

FIG. 7. Three-dimensional waves on a laminar vertical liquid film.

Figure 8 shows experimental heat transfer data in film condensation of water vapours on a vertical tube. Similar data on freon vapour condensation on horizontal tubes are represented in Fig. 9. It is distinctly seen that derivations from the Nusselt theory are practically observed over the total range of Reynolds number and in the $0 < Re < 400$ range the film condensation heat transfer in the laminar wave regime can practically be described by equation (12) with modified coefficients.

The available experimental data in the above range of Re are in the main described by the formula

$$\langle Nu^* \rangle = 0.87\, Re^{-1/4}. \tag{31}$$

In the general case the proportionality factor and the exponent of the Reynolds number of the condensate film are the functions of the Ar^*.

LAMINAR WAVE AND TURBULENT WAVE CONDENSATE FLOWS

Figure 10 illustrates the waves arising in a turbulent liquid film. They are irregular and, to a first approxi-

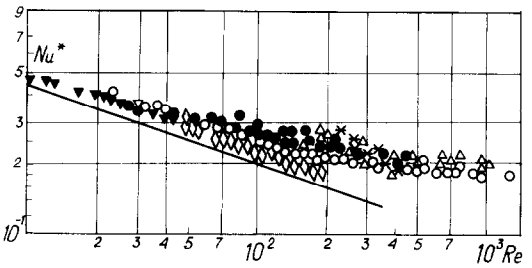

FIG. 8. Experimental data on water vapour condensation on a vertical tube. ○—Kutateladze, Pr = 1.75, Re = 24–1260; △—Meisenburg *et al.*, Pr = 1.7, Re = 115–1000; ●—Zozulya, Pr = 1.75, Re = 27–490; *—Butuzov, Pr = 1.75, Re = 110–435; ◇—Burov, Pr = 1.75, Re = 50–180; ▽—Ratiani, Pr = 1.75, Re = 2.5–44; Solid line—Nusselt calculation.

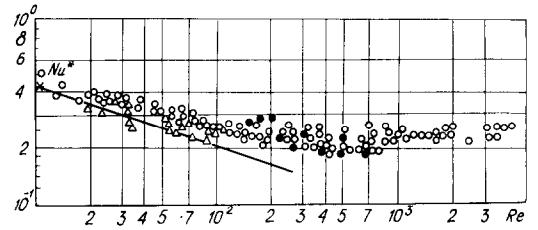

FIG. 9. Experimental data on freon vapour condensation on a vertical tube. ○—Kutateladze and Gogonin, Freon-21, $Pr \approx 3.5$, Re = 10–4250; △—Mazukevich, Freon-12, $Pr \approx 3.5$, Re = 19–100; *—Welt, Freon-12, $Pr \approx 3.5$, Re = 6.8–65; ●—Zozulya, Freon-10, Pr = 4.55, Re = 150–650.

mation, slightly influence the averaged turbulent flow characteristics. They can exert a significant effect in the presence of diffusional resistance on the interphase, e.g. in condensation from vapour–gas mixtures. In condensation of pure non-metal vapours, this resistance is, however, negligible compared with the thermal resistance of the condensate.

Figure 11 illustrates the calculated values $\langle Nu^* \rangle$ in the presence of the laminar wave regime with the heat transfer law (31) in the upper flow region and of the turbulent regime calculated according to the model (24) in its lower region.

Figure 12 represents these dependences sectioned according to the Reynolds numbers of the condensate film. The critical value of the laminar–turbulent transition was taken equal to $Re_{cr} = 400$. According to the above data, it follows that slight variations of this value do not exert a significant influence on $\langle Nu^* \rangle$.

At low Pr the heat transfer quasi-self-similarity is distinctly observed in a rather large range of the supercritical Re.

A comparison of the calculations from the plots in Fig. 12 and experiments with water and Freon-21 vapour condensation (Pr = 1.0–1.7 and 3.5, respectively) is given in Fig. 13. As seen, the data agree well both qualitatively and quantitatively with calculations at $\overline{Pr} \approx 1$ for water vapour and at $Pr \approx 2.5$ for Freon-21, i.e. at $\varepsilon \approx 0.6$–0.7. Therefore, it can be said that the suggested model for the film condensation heat transfer describes qualitatively well a real process and the quantitative agreement is sufficiently readily

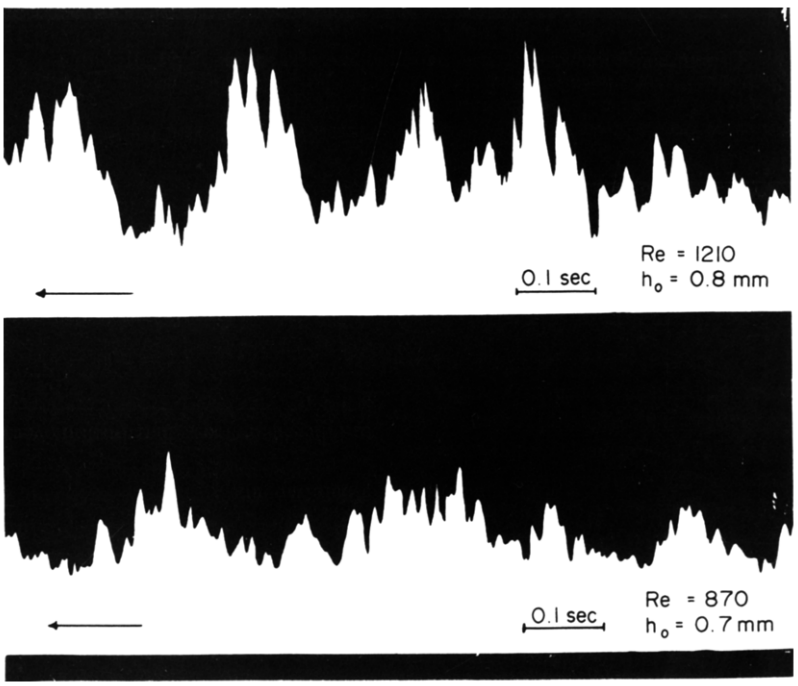

FIG. 10. Photographs of waves on a free vertical turbulent liquid film.

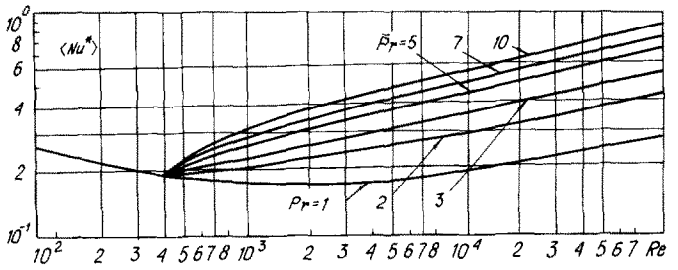

FIG. 11. Dependence of $\langle Nu^* \rangle$ according to (25). Laminar wave region according to (31), turbulent region according to Table 2.

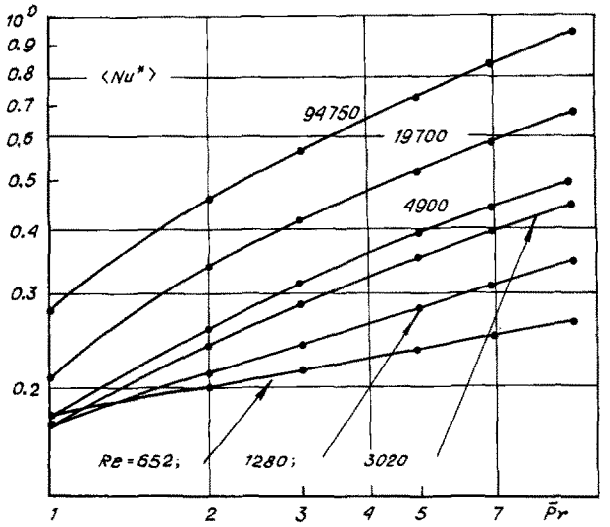

FIG. 12. Sectioned dependence of Fig. 11 according to Reynolds numbers.

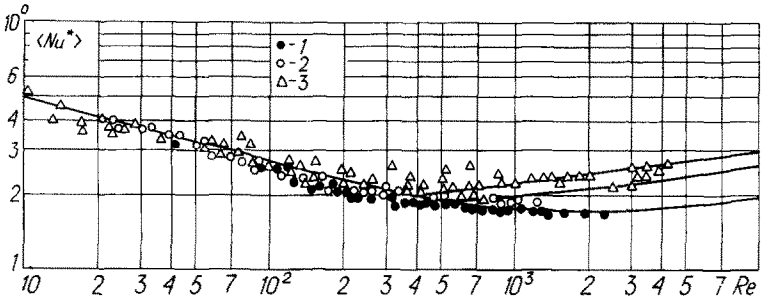

FIG. 13. Comparison of calculations according to the plots in Figs. 11, 12 with experiment for the condensation of water and Freon-21 vapours. $\varepsilon \approx 0.6$–0.7.

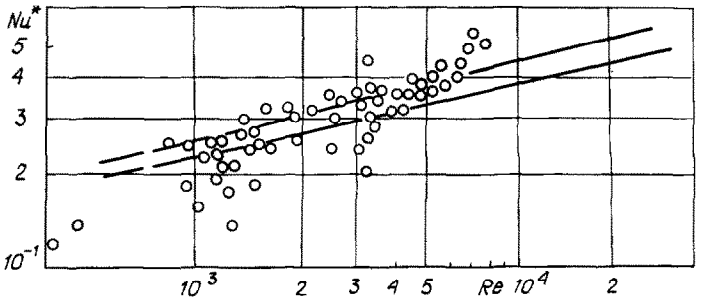

FIG. 14. Diphenyl condensation, $Pr \approx 5.2$. 1—Calculation at $\varepsilon = 1$; 2—calculation at $\varepsilon \approx 0.7$.

realized via the introduction of the ε coefficient, the function (18) being sufficiently weak.

Unfortunately, the literature lacks good experimental data at high Pr of the condensate. A comparison of the suggested calculation with rather obsolete experiments on diphenyl condensation [13] carried out with significant methodological defects is given in Fig. 14. Nevertheless, a definite agreement between theory and experiment is observed here as well.

The considered models are generalized for the condensation of vapour moving parallel to the wall via the introduction of the total V_w^* value (i.e. with taking into account the effect of the gravity force and vapour friction on the interphase).

REFERENCES

1. S. S. Kutateladze, Intrinsic scales in thermohydrogasdynamics, *Int. J. Heat Mass Transfer* **24,** 803 (1981).
2. W. Nusselt, Die Oberflächenkondensation des Wasserdampfers, *Teil* I, II, *Z. VDI* **27,** 541, **28,** 569 (1916).
3. C. G. Kirkbridt, Heat transfer by condensation vapour on vertical tubes, *Ind. engng Chem.* **26,** 425–428 (1934).
4. A. P. Colborn, Calculation of condensation with a portion of the condensate layer in turbulent motion, *Ind. Engng Chem.* **26,** 432–434 (1934).
5. S. S. Kutateladze, *Fundamentals of Heat Transfer.* Academic Press, New York (1963), E. Arnold, London (1963).
6. P. L. Kapitsa, Wave flow of thin layers of viscous liquids, *Zh. Eksp. Teor. Fiz.* **18,** 3–28 (1948).
7. S. S. Kutateladze, V. E. Nakoryakov and B. G. Pokusaev, Experimental investigation of wave processes in gas and vapour–liquid media, in *Proc. Int. Seminar, Dubrovnik, Yugoslavia* (1978).
8. S. V. Alekseenko, V. E. Nakoryakov and B. G. Pokusaev, Waves on the surface of vertical liquid films, Preprint 36–79, Novosibirsk (1979).
9. H. Brauer, Strömung und Wärmeübergang bei Reiselfilmen, *VDI Forschung* **22,** 1–40 (1956).
10. S. S. Kutateladze, The experience in the similarity theory application to the process of heat transfer from condensing saturated vapour, *Zh. Tekh. Fiz.* **7,** 282–293 (1937).
11. S. S. Kutateladze and I. I. Gogonin, Heat transfer in film condensation of slowly moving vapour, *Int. J. Heat Mass Transfer* **22,** 1593–1599 (1979).
12. W. L. Badger, C. C. Monrad and H. W. Diamond, Evaporation of caustic soda to high concentration by means of diphenyl vapours, *Ind. Engng Chem.* **22,** 700–707 (1930).

THÉORIE SEMI-EMPIRIQUE DE LA CONDENSATION EN FILM DE LA VAPEUR PURE

Résume—On considère les modèles les plus simples de la condensation en film de la vapeur non métallique pure et leur correction resultant de l'analyse des resultats d'experience disponibles.

HALBEMPIRISCHE THEORIE DER FILMKONDENSATION DES REINDAMPFES

Zusammenfassung—Es werden betrachtet die einfachsten mathematischen Modelle der Filmkondensation des reinen Nichtmetalldampfes und ihre Korrektion, die aus der Analyse der vorhandenen Versuchsergebnisse hervorgeht.

ПОЛУЭМПИРИЧЕСКАЯ ТЕОРИЯ ПЛЕНОЧНОЙ КОНДЕНСАЦИИ ЧИСТОГО ПАРА

Аннотация — Рассматриваются простейшие математические модели пленочной конденсации чистого неметаллического пара и их корректировка, следующая из анализа имеющихся экспериментальных данных.